Sensor Review, Sensor Review, Vol.36 Iss 3 pp. 303 – 311 (Final manuscript)

The Latest Trend in Nano-bio sensor Signal Analysis

Teh Yi Jun[1], Asral Bahari Jambek[2] and Uda Hashim[3]
[1,2]*School of Microelectronic Engineering, Universiti Malaysia Perlis, Perlis, Malaysia*
[3]*Insituite of Nano Electronic Engineering, Universiti Malaysia Perlis, Perlis, Malaysia*
Email: [1]kelvinteh90@gmail.com, [2]asral@unimap.edu.my, [3]uda@unimap.edu.my

***Abstract*—This paper discusses a nanoscale biosensor and its signal analysis algorithms. In this work, five nanoscale biosensors are reviewed, which namely silicon nanowire FET biosensors, polysilicon nanogap capacitive biosensors, nanotube amperometric biosensors, gold nanoparticle-based electrochemical biosensors and quantum dot-based electrochemical biosensors. Each biosensor produces a different output signal depending on their electrical characteristics. Five signal analysers are studied, with most of the existing signal analyser analysis based on the amplitude of the signal. Based on the analysis, auto-threshold peak detection is proposed for further work.**

***Index Terms*—Nano-bio sensor; Bio sensor signal analysis.**

1. INTRODUCTION

Over the past decade, nano-technologies have grown rapidly. This take the advantages of nanoscale biosensors to improve their sensitivity due to their suitable properties. Nano structures, such as nanogaps, nanowires, nanoparticles, nanotubes, nanoscale films and quantum dots(QDs), are implemented in biosensors to produce nanoscale biosensors.

The signal of nanoscale biosensors can be analysed in terms of amplitudes, phases, frequencies and delays. Hence, an efficiency signal analysis algorithm is required to support the growth of nanoscale biosensors. Under the conventional method, signal analysis is performed by a human using an off-chip device. This approach has the potential to lead to human, error, and is expensive, time consuming and not suitable for portable lab-on-chip applications. With the growth of system-on-chip (SoC) technology, it is possible to develop on-chip analyzer for nano-biosensors.

2. NANO-BIO SENSORS

In this section, the latest nano-biosensor will be reviewed. The operation of the device will be discussed and the electrical signal output from the sensor will be highlighted. The authors in [1], [2] proposed silicon nanowire field-effect-transistor (SiNW-FET) -based biosensors for highly selective, sensitive, label-free and real-time measurements. Fig. 1 illustrates the working system and principle of the SiNW-FET-based biosensor. SiNW-FET-based biosensors consist of drain, source and gate electrodes. The drain and source electrodes function as the bridgeheads of the semiconductor device channel, which allows the current to flow from the source to drain. In the SiNW-FET-based system, the biological receptors were anchored on the surface of the silicon nanowires to recognize target analytes. When the target was bound by receptors, the surface potential underwent changes and the channel conductance was modulated. Fig. 2 illustrates the results of SiNW-FET both without and with the designed receptor for uncharged steroid concentration measurements. From the graph, we can see that the SiNW-FET with the designed receptor will increase conductance, while the concentration of 19-NA increases; however, for the SiNW-FET without the designed receptor, the conductance remains the same while the concentration of 19-NA increases.

The authors in [3], [4] proposed polysilicon nanogap capacitive biosensors. Fig 3 illustrates the nanogap cavity using SEM. The fabrication of the biosensor involves using the conventional simple dry oxidation process and the lithographic process. Nanoscale dielectric spectroscopy was used between the nanogap patterns to measure the potential of hydrogen (pH) value. The device was used to study the capacitance-frequency (C-F) relationship and the capacitance-voltage (C-V) relationship. Fig. 4 shows the C-F relationship and the C-V relationship. The results show that the lowest gap-value for the nanogap structure will provide better sensitivity of pH detection. This is due to the C-V and C-F characteristics of the device.

The authors in [5]–[7] proposed an amperometric biosensor based on tyrosinase (Ty)/carboxyl functionalized single-walled carbon nanotubes (SWCNTs) and a modified carbon screen-printed electrode (SPE) for tyramine detection. The biosensor is used for assaying tyramine in fish products. Fig. 5 illustrates the enzymatic reactions of tyramine in the presence of tyrosinase. Fig. 6 illustrates the response of the sensors to the tyramine, while Fig. 7 shows the influence of the pH value on the biosensor response. The biosensor has good linearity, with the concentration of tyramine within the range of five–180 microM, with a sensitivity of 0.7414 A x M^{-1} for the optimal conditions and a detection limit of 0.62 microM.

Published manuscript link: http://dx.doi.org/10.1108/SR-08-2015-0132

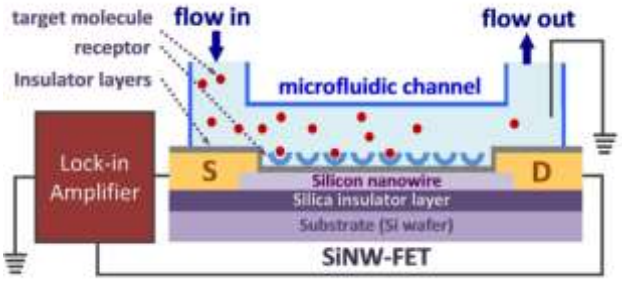

Fig. 1. The working system and principle of the SiNW-FET biosensor [1].

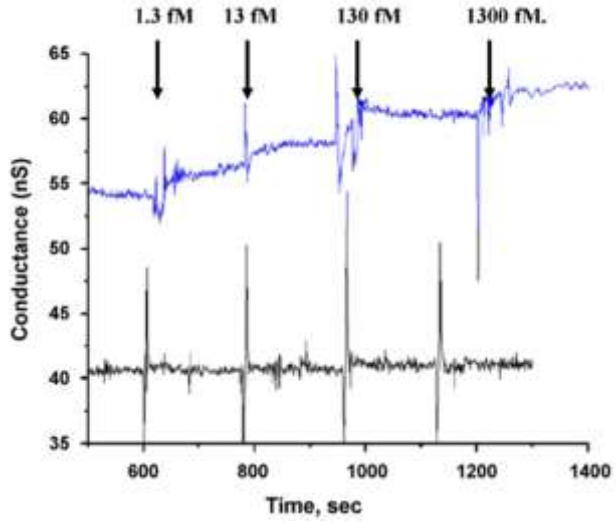

Fig. 2. Real-time of recording the conductance response in the presence of 19-norandrostenedione (19-NA) by a SiNW-FET with (blue line) or without (black line) the designed receptors [1].

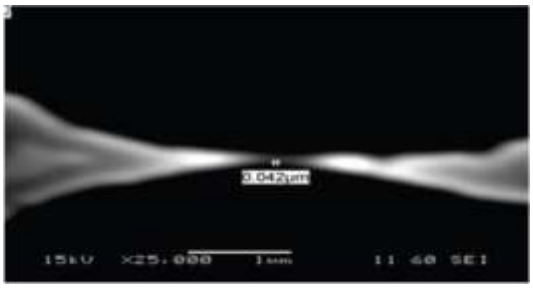

Fig. 3. SEM by JEOL: device A shows a nanogap cavity at 42nm using an in-testing pH sample [3].

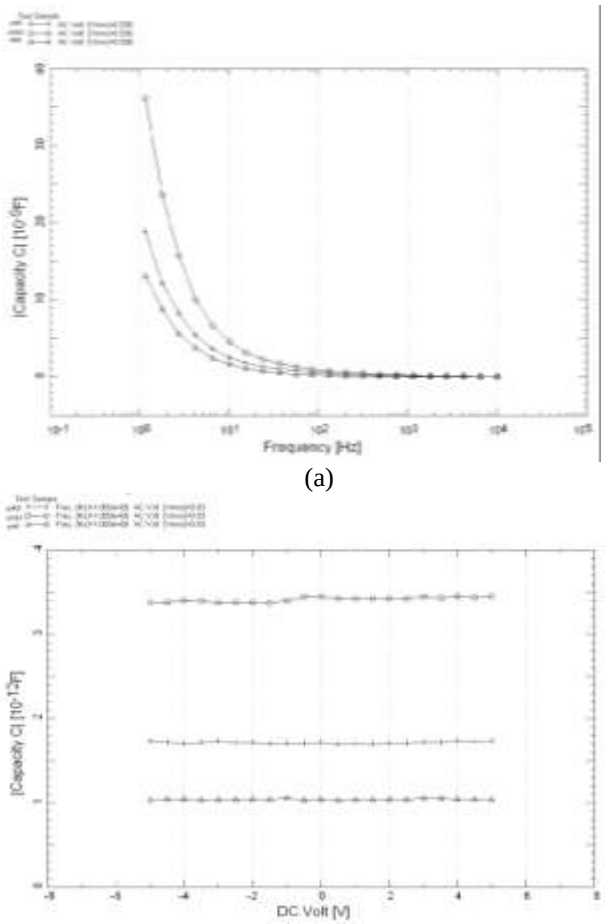

(a)

(b)

Fig. 4. (a) Capacitance-Frequency relationship of 3, 5 and 10 of different types of pH; (b) Capacitance-Voltage relationship of 3, 5 and 10 of different types of pH [3].

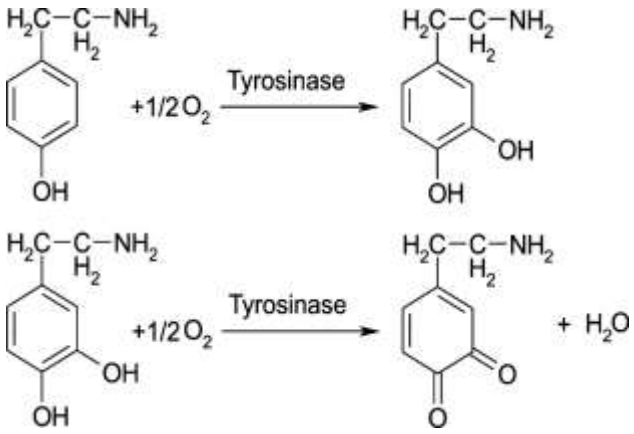

Fig. 5. Enzymatic reactions of tyramine in the presence of tyrosinase [5].

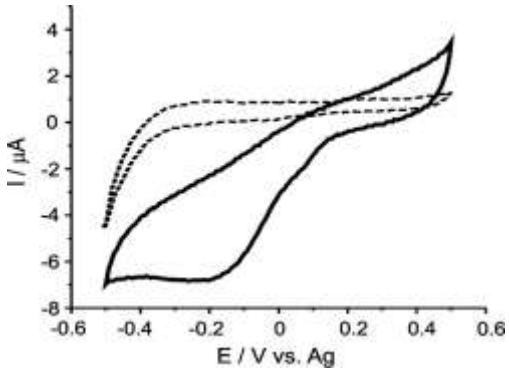

Fig. 6. Cyclic voltammograms of the Ty-SWCNT-COOH/SPE biosensor in the absence (dashed line) and presence of 100 microM tyramine (solid line) [5].

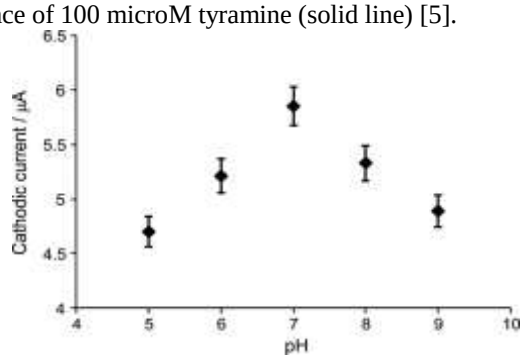

Fig. 7. The influence of the pH value in the biosensor response [5].

Fig. 8. Schematic illustration of the colloidal AuNPs-based electrochemical detection system [8].

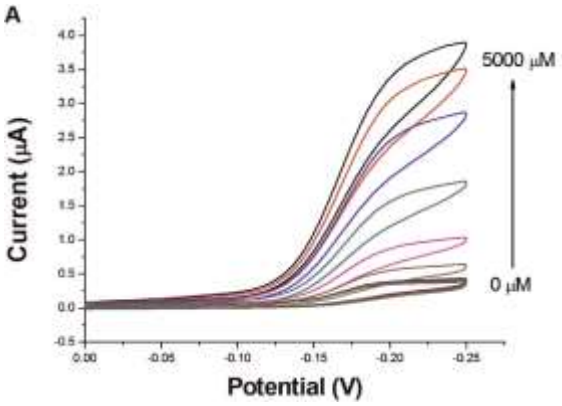

Fig. 9. Cyclic voltammograms obtained upon analysing different concentrations of glucose [8].

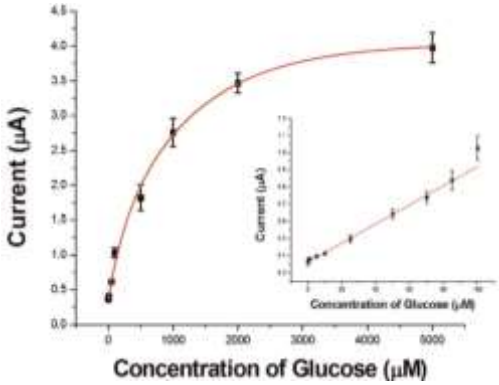

Fig. 10. Relationship between the peak currents at -0.25 V and the concentrations of glucose. The inset shows a linear relationship in a concentration range from 0 mM to 100 mM [8].

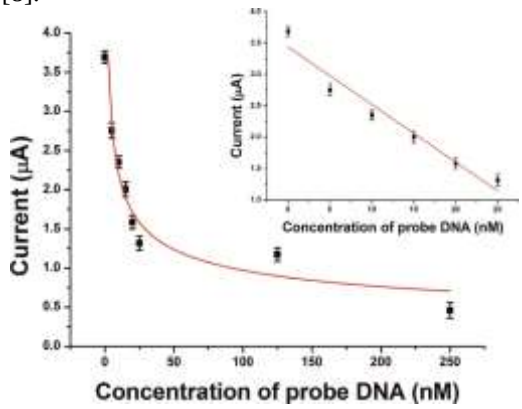

Fig. 11. The calibration curve of the cyclic voltammetric peak currents against the concentrations of the probe DNA [8].

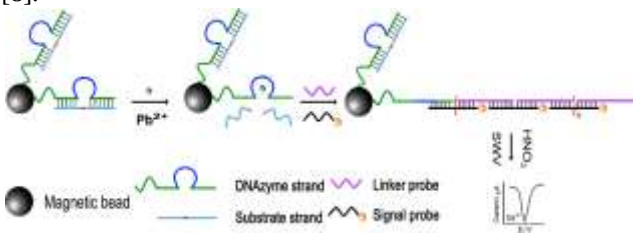

Fig. 12. The principle of the cascade DNA-based electrochemical sensing system for Pb^{2+} detection [9].

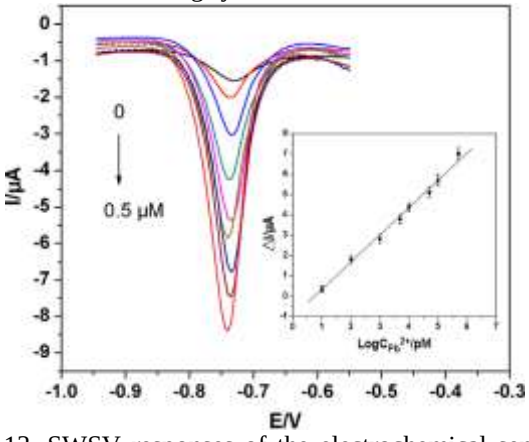

Fig. 13. SWSV responses of the electrochemical sensing system for Pb^{2+} at various concentrations [9].

The authors in [8], [10] proposed the direct application of gold nanoparticle-based electrochemical biosensors to detect the concentration of glucose. In this biosensor, the colloidal AuNPs are adopted directly as the electrolyte, unlike in the conventional case which is only immobilized on the surface of the electrodes. Fig. 8 illustrates the colloidal AuNPs-based electrochemical detection system. The sensitive detection of the glucose is tested and the results are show in Fig. 9, which can fitted by an equation: $Y = 0.3633 + 0.00558X$ ($R^2 = 0.98$), with a detection limit of 1 mM as show in Fig. 10. Another experiment have been done to show that single-nucleotide polymorphism can be detected using this device. The results are show in Fig. 11, which shows that a linear relationship between the current and the concentration of the target DNA is also obtained with a linear equation: $Y = 2.0445 + 0.0897X$ ($R^2 = 0.99$). Hence, the results clearly show that the target DNA and the 1-base mismatched variant can be achieved for this device.

The authors in [9], [11] proposed to develop an ultrasensitive electrochemical Pb^{2+} biosensor which cascades DNA and QDs. The sensitivity and selectivity was tested in the experiments. Fig. 12 illustrates the principle behind the device. In the absence of Pb^{2+}, the substrate strand could not be cleaved. In contrast, in the presence of Pb^{2+}, it is able to cleave the substrate strand into two DNA fragments at the ribonucleotide site. A free catalytic strand is released due to a lack of thermal stability. One terminus of the signal probe is hybridized with the free catalytic strand, while the other terminus hybridized with the linker probe. A long DNA concatemer containing numerous alternating signal probes and linker probes can be formed by continuous hybridization, and can also be assembled with numerous QDs. As a result, a remarkably amplified electrochemical signal can be obtained. Fig. 13 show a linear range was achieved from10.0 pM to 500.0 nM with a detection limit of 6.1 pM. Based on the results, this shows that the sensor achieves a linearity relation for its current different from the Log concentration of Pb^{2+}.

Table 1: Summaries of Sensors

Sensors	[1], [2]	[3], [4]	[5]–[7]	[8], [10]	[9], [11]
Nano structures	Nanowire	Nanogap	Nanotu-be	Nanopartil-ces	Quantum dot
Bio application	19-NA	pH	Tyrami-ne	Glucose	DNA
Respond	Conducta-nce	Capacita-nce	Current	Current	Current
Input	-	Voltage and Frequency	Voltage	Voltage	Voltage
Relations	Linear	Linear	Linear	Linear	Linear

3. SIGNAL ANALYSIS

In this section, we will discuss several methods for how the sensor signal is to be processed. Four main signal changes due to the sensor reaction are discussed, namely amplitude, time, frequency and phase. The authors in [12] proposed a peak detection algorithm for portable multi-model nano-biosensor system. The peak detection is an important step for signal processing applications. The author in [13] proposed auto-threshold peak detection which is suitable to apply with a micro-controller due to its simplicity. Fig. 15 illustrates the peak detection of the noise signal using the auto-threshold algorithm. This algorithm consists of two stages which are a threshold calculation stage and a peak detection stage. In the threshold calculation stage, the threshold value of the signal will be estimated with a terminated condition. In the peak detection stage, the peak detection will be performed using the threshold value calculated by the previous stage.

The authors in [14] proposed a bio-signal processor platform using an SoC approach. In the bio-signal processing part, the raw bio-signal is filtered first to reduce the noise, before comparing it with reference bio-signal database (DB). Fig. 16 illustrates the 'compare and accept' method. As the measured signal is compared against the reference signal, the signal which has most similar properties to the reference signal is accepted. Using this method, and if we already have the aptamer disease data, we can detect the disease using this method.

The authors in [15] proposed a time-frequency algorithm using a synchrosqueezing transform and the concept of joint instantaneous frequency multivariate data. The raw signal will be involved in modulation. The synchrosqueezing transform is used to produce time-frequency representations of non-stationary signals. The instantaneous frequencies of the synchrosqueezed coefficients are determined for each oscillatory scale, and the resulting multivariate instantaneous frequency is then founded by calculating the joint instantaneous frequency of each oscillatory scale across the channels. The drift velocities along the latitude and longitude shown in Fig. 17(a) contain a time-varying oscillation that is common to both channels; however, these oscillations are not in phase. The noise in both channels also had different characteristics. Fig. 17(b) illustrates that the common oscillatory dynamics of the float drift data that is frequency modulated are effectively localized using the proposed method, while the multivariate pseudo-Wigner distribution had poorer localization.

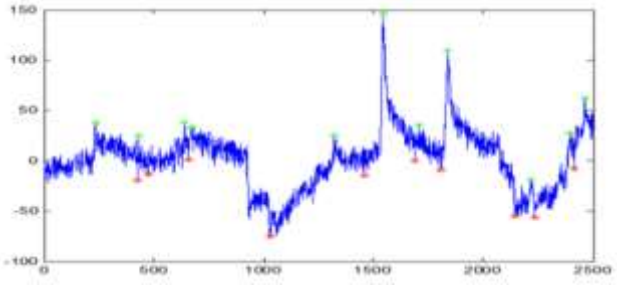

Fig. 15. Peak detection results of the auto-threshold algorithm [12].

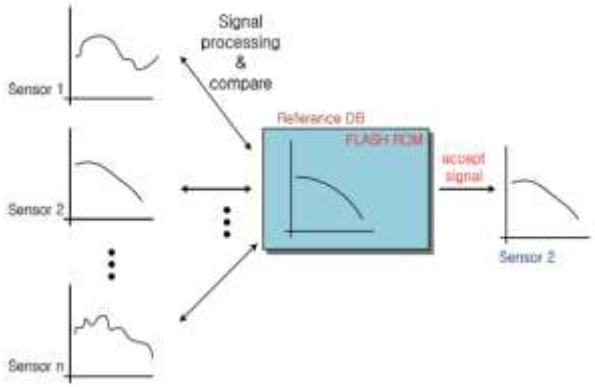

Fig. 16. The compare and accept method [14].

Fig. 17. Time-frequency analysis of real-world float drift data. (a) The time-domain w

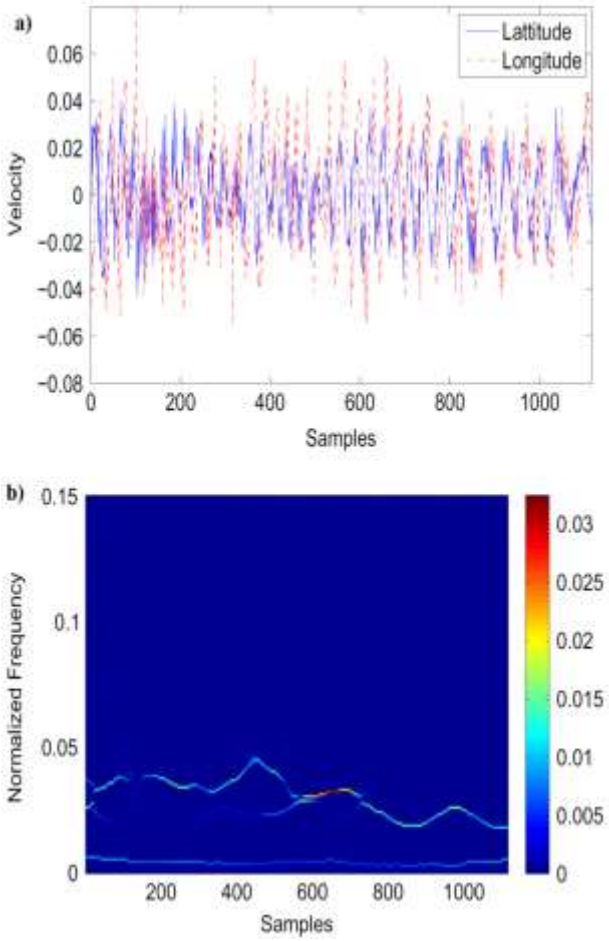

aveforms of bivariate float-velocity data. (b) The time-frequency representation of the float data using the proposed multivariate extension of the SST [15].

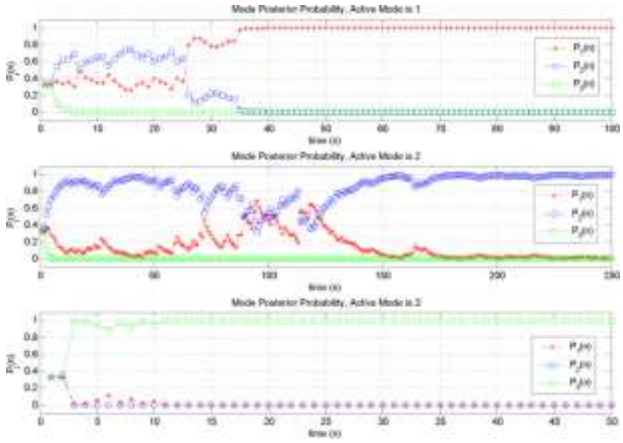

Fig. 18. Posterior probability transient. It can be seen that $\lim_{n\to\infty} P_{\text{active mode}}(n) = 1$ for all possible active modes. Empirical measurements produced according to a possible mode of the system are used in the classification algorithm. [16]

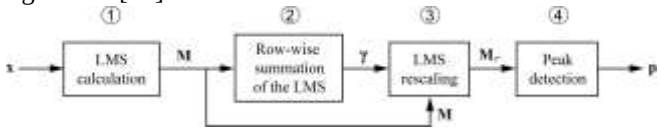

Fig. 19. Calculation steps of the AMPD algorithm [17].

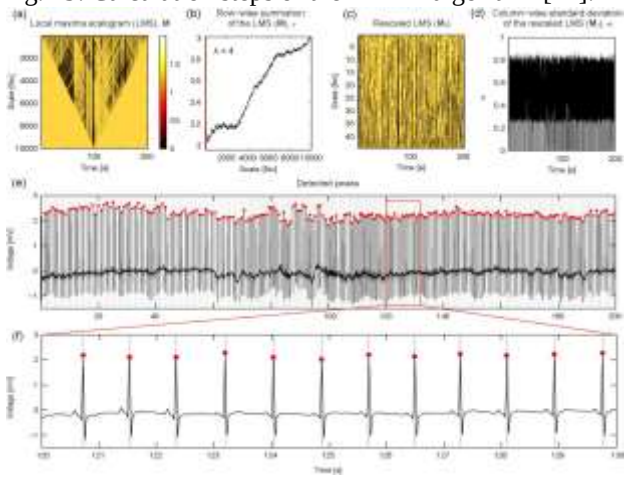

Fig. 20. Results of applying the AMPD algorithm to an ECG time series [17].

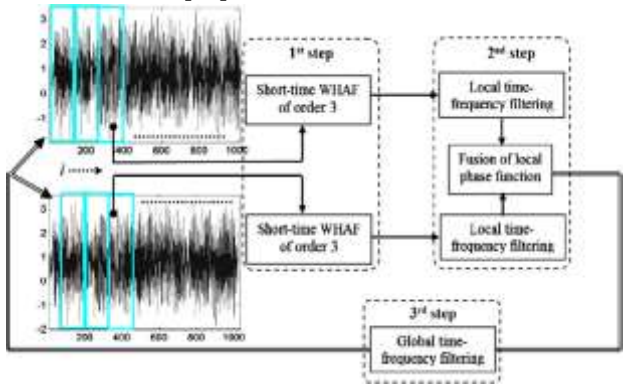

Fig. 21. Synoptic scheme of a time-frequency-phase analyser with the three steps of the algorithm: short-time

polynomial phase modelling, fusion, and component extraction [18].

The authors in [16] proposed the stochastic modelling and signal processing of nano-scale protein-based biosensors. With the presence of analyte in the electrolyte, the current or resistance of the device will change. The chemical dynamics of the biosensor's response to the analyte concentration are modelled by a two-timescale nonlinear system of differential equations. The system used the Kalman filter in the multiple model adaptive estimation (MMAE) algorithm to estimate the concentration of the analyte, which classified the level of concentration as null, medium or high from the noisy measurement from the biosensor. Fig. 18 illustrates the response of the classification algorithm to empirical measurements of the channel conductance when the analyte and the binding site are, respectively, Streptavidin and Biotin. As shown, the algorithm performs well in detecting the active mode of the system when real data are used. In each of the subplots of Fig. 18, the channel conductance is evolving according to one of three possible regimes, depending on the analyte concentration. It can be seen that, as expected, the probability of each of the models except for the true model approaches 0, while the probability of the true model approaches 1.

The authors in [17] proposed automatic multiscale-based peak detection (AMPD) for a quasi-periodic and noisy periodic signal. The algorithm consists of calculating the local maxima scalogram (LMS), comprising a row-wise summation of the LMS matrix M, reshaping the LMS matrix M, and peak-detection. Fig. 19 illustrates the calculation steps of the AMPD algorithm. The AMPD was applied in a few real-world signals, like sunspot numbers, the blood volume pulse in fNIRS signals, and QRS peaks in ECG signals. Fig. 20 illustrates the results of applying the AMPD algorithm to an ECG time series. The results show that all the R-peaks of the ECG signal are detected. Base on the results the authors find that the AMPD is available to use and test the algorithm in real-world applications.

The authors in [18] proposed a time-frequency-phase tracker to analyse the underwater mammal vocalizations. This method consists of three steps, which are short-time analysis, selection and fusion, and component extraction. In the short-time analysis step, time windowing and a third-order windowed high-order ambiguity function (WHAF) is applied to the signal to reduce the dependence of polynomial modelling on the window size. In the selection and fusion step, frequency filtering and a fusion procedure is applied to the signal in order to extract the signal's samples corresponding to the time-frequency regions defined in the neighbourhood of the local functions. Next is the component extraction step – the remaining signal is fed back to the input of the first step. The process is repeated until all the components of interest have been extracted. Fig. 21 illustrates the synoptic scheme of the time-frequency-phase analyser.

4. DISCUSSIONS

Table 2: Comparisons of signal analysis algorithms.

Algorithms	[12], [13]	[14]	[15]	[16]	[17]	[18]
Signal periodic	None	None	None	None	periodic or quasi-periodic	None
Analysis based	time-amplitude	amplitude	time-frequency	amplitude	time-amplitude	time-frequency-phase
Pre-process data	NA	filtering	modulation	Kalman filter	Window-moving	time windowing, WHAF
Signal analysis	peak detection	compare	frequency detection	multi-hypothesis	peak detection	time-frequency tracking
Complexity	simple	simple	complex	complex	complex	complex

In this section, we will discuss the suitability of each method presented in section 3 for use in an automatic nano-biosensor system. The bio-signal can be analysed based on the change in amplitude, phase, frequency or delay. The auto-threshold peak-detection proposed by [12] is simple and automatic. Hence, it is suitable to be applied to SoC. The compare and accept method proposed by [14] is suitable for application during the classification stage. The method proposed by [16] is only suitable for the specific sensor design, because the analyser is designed base on the specified chemical dynamics on the sensors. The AMPD proposed by Scholkmann [17] is not suitable for application in the automatic nano-biosensor analyser for analyses the amplitude of the signal due to it does not applicable to non-periodic signal. Based on the review, there are few kinds of response to electrical output from the sensor, namely amplitude, phase, time and frequencies. Hence, only the amplitude is analyses was not enough information to classified the bio signal. To obtain more accurate and useful information from the bio-signal, the phase-, frequency- and time-analysis must be implemented into the auto-threshold peak-detection.

5. CONCLUSIONS

In this paper, five nanoscale biosensors were reviewed. Each sensor produces different wave signals due to the electrical characteristics. Most of the electrical signals can be classified based on the amplitudes, phases, frequencies and delays. Five signal analysers were also studied. Most research has focused on peak detection. To increase the accuracy of the analyser for the nano-biosensor, phase-, frequency- and delay-analysis must be implemented in the peak-detection analyser.

6. ACKNOWLEDGEMENTS

This research was supported by the Fundamental Research Grant Scheme, Ministry of Higher Education, Malaysia (FRGS Phase 1, 2014).

REFERENCES

[1] M.-Y. Shen, B.-R. Li, and Y.-K. Li, "Silicon nanowire field-effect-transistor based biosensors: from sensitive to ultra-sensitive.," *Biosens. Bioelectron.*, vol. 60, pp. 101–11, Oct. 2014.

[2] B.-R. Li, C.-W. Chen, W.-L. Yang, T.-Y. Lin, C.-Y. Pan, and Y.-T. Chen, "Biomolecular recognition with a sensitivity-enhanced nanowire transistor biosensor.," *Biosens. Bioelectron.*, vol. 45, pp. 252–9, Jul. 2013.

[3] N. Taib, U. Hashim, A. Saifullah, T. S. Dhahi, and J. K. Setar, "Polysilicon Nanogap capacitive biosensors for the pH detection," *IEEE Reg. Symp. Micro Nanoelectron.*, vol. 1, pp. 250–252, 2011.

[4] T. S. Dhahi, U. Hashim, M. E. Ali, and N. Taib, "Polysilicon nanogap fabrication using a thermal oxidation process," *Microelectron. Int.*, vol. 29, no. 1, pp. 40–46, Jan. 2012.

[5] I. M. Apetrei and C. Apetrei, "The biocomposite screen-printed biosensor based on immobilization of tyrosinase onto the carboxyl functionalised carbon nanotube for assaying tyramine in fish products," *J. Food Eng.*, vol. 149, pp. 1–8, Mar. 2015.

[6] I. M. Apetrei and C. Apetrei, "Biosensor based on tyrosinase immobilized on a single-walled carbon nanotube-modified glassy carbon electrode for detection of epinephrine.," *Int. J. Nanomedicine*, vol. 8, pp. 4391–8, Jan. 2013.

[7] I. M. Apetrei, M. L. Rodriguez-Mendez, C. Apetrei, and J. a. de Saja, "Enzyme sensor based on carbon nanotubes/cobalt(II) phthalocyanine and tyrosinase used in pharmaceutical analysis," *Sensors Actuators B Chem.*, vol. 177, no. 2013, pp. 138–144, Feb. 2013.

[8] G. Chen, H. Tong, T. Gao, Y. Chen, and G. Li, "Direct application of gold nanoparticles to one-pot electrochemical biosensors.," *Anal. Chim. Acta*, vol. 849, pp. 1–6, Nov. 2014.

[9] S. Tang, W. Lu, F. Gu, P. Tong, Z. Yan, and L. Zhang, "A novel electrochemical sensor for lead ion based on cascade DNA and quantum dots amplification," *Electrochim. Acta*, vol. 134, pp. 1–7, Jul. 2014.

[10] X. Zhu, M. Liu, H. Zhang, H. Wang, and G. Li, "A chemical approach to accurately characterize the coverage rate of gold nanoparticles," *J. Nanoparticle Res.*, vol. 15, no. 9, p. 1900, Aug. 2013.

[11] S. Tang, P. Tong, H. Li, J. Tang, and L. Zhang, "Ultrasensitive electrochemical detection of Pb^{2+} based on rolling circle amplification and quantum dots tagging.," *Biosens. Bioelectron.*, vol. 42, no. 2013, pp. 608–11, Apr. 2013.

[12] J. Park, J. Song, H. Kim, and D. Ryu, "Peak Detection for Portable Multi-modal Nano-bio Sensor System," *Int. J. Bio-Science Bio-Technology*, vol. 5, no. 3, pp. 135–142, 2013.

[13] a. L. Jacobson, "Auto-threshold peak detection in physiological signals," *2001 Conf. Proc. 23rd Annu. Int. Conf. IEEE Eng. Med. Biol. Soc.*, vol. 3, pp. 2194–2195, 2001.

[14] D. Lee, S. Jung, Y. Par, J. Xu, and J. Par, "Bio-signal Procssor Platform System For Array Sensors," *IEEE Int. Conf. Bioinforma. Biomed. Work.*, pp. 904–906, 2011.

[15] A. Ahrabian, D. Looney, L. Stanković, and D. P. Mandic, "Synchrosqueezing-based time-frequency analysis of multivariate data," *Signal Processing*, vol. 106, pp. 331–341, Jan. 2015.

[16] S. M. Monfared, V. Krishnamurthy, and B. Cornell, "Stochastic modeling and signal processing of nano-scale protein-based biosensors," *2009 IEEE Int. Work. Genomic Signal Process. Stat.*, pp. 1–6, May 2009.

[17] F. Scholkmann, J. Boss, and M. Wolf, "An Efficient Algorithm for Automatic Peak Detection in Noisy Periodic and Quasi-Periodic Signals," *Algorithms*, vol. 5, no. 4, pp. 588–603, Nov. 2012.

[18] C. Ioana, C. Gervaise, Y. Stéphan, and J. I. Mars, "Analysis of underwater mammal vocalisations using time–frequency-phase tracker," *Appl. Acoust.*, vol. 71, no. 11, pp. 1070–1080, Nov. 2010.